Mansoura Engineering Journal

Volume 49 | Issue 5 Article 12

2024

Effect of rasp heads with an equivalent height of end sill on scour hole dimensions downstream weirs

Hadeer Abdelati
Civil Engineering, 2012, Faculty of Engineering, Mansoura University, Egypt., hadeerabdelati7@gmail.com

A.A. El-Masry
Prof. of Irrigation and Hydraulics Engineering Dept., Civil Engineering, Faculty of Engineering, Mansoura University

M.T Shamaa
Associate. Prof. of Irrigation and Hydraulics Engineering Dept., Civil Engineering, Faculty of Engineering, Mansoura University

K.A Nassar
Assistant Professor in Irrigation Engineering and Hydraulics Department, Civil Engineering, Faculty of Engineering, Mansoura University

Recommended Citation

Abdelati, Hadeer; El-Masry, A.A.; Shamaa, M.T; and Nassar, K.A (2024) "Effect of rasp heads with an equivalent height of end sill on scour hole dimensions downstream weirs," *Mansoura Engineering Journal*: Vol. 49 : Iss. 5 , Article 12.
Available at: https://doi.org/10.58491/2735-4202.3231

ORIGINAL STUDY

Effect of Rasp Heads With an Equivalent Height of End Sill on Scour Hole Dimensions Downstream of Weirs

Hadeer Abdelati [a,*], Adel A. El-Masry [b], Mohamed T. Shamaa [b], Karim A. Nassar [c]

[a] Departments of Civil Engineering, Faculty of Engineering, Mansoura University, Mansoura, Egypt
[b] Department of Irrigation and Hydraulics Engineering, Faculty of Engineering, Mansoura University, Mansoura, Egypt
[c] Department of Irrigation Engineering and Hydraulics, Faculty of Engineering, Mansoura University, Mansoura, Egypt

Abstract

The occurrence of local scour downstream of heading-up structures poses a significant threat to their safety and stability, leading to complete failure. In this study, a series of 96 experiments were conducted in a rectangular flume downstream of a Fayoum-type weir. The experiments were designed to investigate the effects of various flow conditions, including a wide range of Froude numbers and tailwater depths. Three different applied discharges of 17.29, 20.63, and 24.17 l/s were used, along with 12 values of the Froude number ranging from 0.19 to 0.39. Experimental runs were divided into three distinct groups. The first group comprised 12 runs conducted on a flat floor without any energy dissipation devices. The second group consisted of 48 runs on a flat floor that ended with a sill. The third group encompassed 36 runs on a flat floor with rasp heads, examining the effectiveness of an equivalent height to the most effective height of the end sill in reducing scour. Rasp heads were positioned in three different locations. The results of the experiments showed that the best height of the end sill was $h_s = 0.05H_s$ where it reduced scour parameters by 37.5−83% for scour depth and from 3.48 to 43.48% for scour length. The best position for the rasp heads was at the first one-third of the floor length. In this position, the scour depth and length were reduced by 55.28−96.43% and from 44.44 to 85.7%, respectively, compared with scour depth and length on a flat floor.

Keywords: End sill, Froude number, Heading-up structures, Local scour, Rasp heads

1. Introduction

Weirs are overflow hydraulic structures used to control water flow in rivers, streams, and other water bodies. Weirs have been used for many centuries by hydraulic engineers for a variety of purposes, including flood control, water measurement, industrial purposes, distribution of water between canals for irrigation, reducing the water slope in canals, excluding sediments, and regulation of flow depth (Abozeid *et al.*, 2010; Alabas *et al.*, 2017; Amin, 2015; Elnikhely and Fathy, 2020; Obaida *et al.*, 2023).

A diverse array of weirs exists globally, each exhibiting unique characteristics and engineering designs. Among these, clear overfall weirs emerge as prevalent structures within the irrigation systems of Egypt, particularly in the renowned Fayoum region. The term "Fayoum standard weir" has gained international recognition, highlighting its widespread reputation and influence in hydraulic engineering practices worldwide.

Weirs' design principles and considerations include hydraulic performance, structural integrity, management, safety, maintenance, availability, integration with the surrounding environment, and compliance with regulations. Several factors can contribute to the erosion or removal of sediments from the channel bed downstream of a weir structure, known as local scour. It is a common

Received 3 May 2024; revised 10 June 2024; accepted 20 June 2024.
Available online 5 September 2024

* Corresponding author at: Faculty of Engineering, Mansoura University, Egypt.
E-mail address: hadeerabdelati7@gmail.com (H. Abdelati).

https://doi.org/10.58491/2735-4202.3231

morphological issue that can influence the stability of weirs and other hydraulic structures causing the failure of these structures (Amin, 2015; Abdelhaleem, 2013; Bormann and Julien, 1991; Chaudhary *et al.*, 2022; D'agostino and Ferro, 2004; Hamed *et al.*, 2009; Zahed *et al.*, 2010). The prediction of local scour downstream of weirs remains a challenge. Despite many studies into scouring processes, accurately estimating the exact dimensions of scour holes downstream of hydraulic structures remains a difficult problem. Minimizing scour holes were studied downstream sharp-crested weir using a solid apron with different lengths (Obaida *et al.*, 2023; Hong *et al.*, 2015; Varaki *et al.*, 2022). Results showed that increasing the length of the solid apron reduces scour holes. However, expanding the length of the floor behind the structure results in a heightened susceptibility to increased uplift force. This requires increasing the thickness of the concrete floor, consequently raising the overall costs of the structure.

Among the most common mitigation techniques to reduce scour hole dimensions are stilling basins that are used to protect the region downstream of hydraulic structures, especially downstream low-heading structures, such as weirs, spillways, and dams from excessive scouring. They help in the dissipation and absorption of flow energy, reducing erosion forces on the riverbed. Also, they are built for economic reasons by reducing the total length of the hydraulic jump on the established apron and changing the jump characteristics to achieve better performance in shorter lengths. The jump length can be reduced by installing baffles and sills in the stilling basin. Local scour downstream of adverse stilling basins caused by a submerged wall jet released by a sluice gate was studied (Farhoudi and Shayan, 2014). The results demonstrated that as the stilling basin's length and slope increased, the scour hole's maximum depth decreased. Alaa *et al.* (2021) also examined the impact of different stilling basin pool locations and sizes on the submerged jump downstream sluice gate hydraulic structures. The results demonstrated minimizing scour depth and achieving maximum energy dissipation. A stilling basin's hydraulic design must reduce the size and cost of the structure.

Sills are essential components that are frequently used in the design of stilling basins and weirs to dissipate the energy of the water flowing downstream of the structure by changing the direction and velocity of the flow. This decreases the kinetic energy and prevents excessive erosion. Experimental runs were carried out under varying flow conditions on sills fixed in the floor of a flume downstream heading-up structures with different heights. Results demonstrated that sill heights decrease scour holes and effectively affect energy dissipation (Abdallah, 1990; Alikhani *et al.*, 2010; Awaad, 2023; Hamidifar *et al.*, 2018; Helal *et al.*, 2013). The impact of V-notch end sill overstepped spillways on energy dissipation and scour downstream of spillways was examined (El-Mahdy, 2021). The results showed that all V-notch end sill angles reduced the relative scour length, depth, and volume, and increased energy dissipation. Experimental research on the impact of semicircular sills on the hydraulic jump and scour hole was conducted by Abdel Samad *et al.* (Abdel *et al.*, 2012). They demonstrated the sill's recommended shape decreased the size of the scour hole and the hydraulic jump.

Baffles are hydraulic engineering structures used to control the flow of water and reduce the scouring effect downstream of hydraulic structures. They are commonly installed in stilling basins as energy dissipators downstream of heading-up structures to dissipate the energy of flowing water and prevent erosion and scouring. The configuration and morphology of baffles block wield significant influence on the scouring phenomenon occurring downstream of a weir. To comprehensively examine the impact of different arrangements and shapes of baffles, numerous experimental investigations using various types and configurations of baffles on the apron were conducted as depicted in Fig. 1. These studies aimed to assess the effects of diverse baffle block arrangements and shapes on both scour depth and energy dissipation, to identify the optimal configuration for minimizing the dimensions of scour holes downstream of structures characterized by upstream-facing orientations. Notable research contributions in this domain (El-Masry and Sarhan, 2000; El-Gamal, 2001; El-Masry, 2001; Wang *et al.*, 2017), who explored the implementation of single, double, and triple lines of angle baffles featuring vertical faces to mitigate the scouring effects of downstream hydraulic structures. They concluded with the following recommendations:

(1) The optimum block front face should be vertical and perpendicular to the flow direction.
(2) The row of the baffle blocks in the first one-third of the floor length is more efficient in reducing scour hole dimensions than the second row.
(3) The floor baffle blocks should occupy between 40 and 55% of the width of the floor.
(4) The fully baffled floor is suitable for all flow conditions during operation conditions.

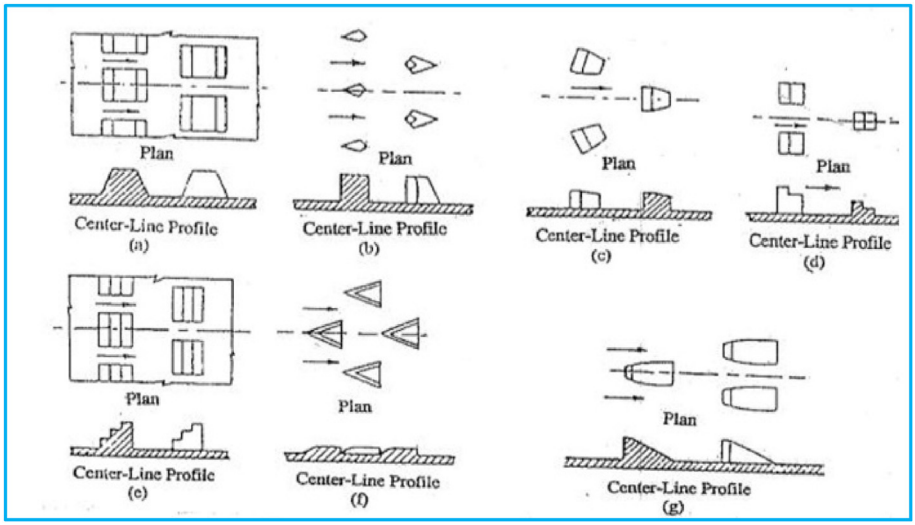

Fig. 1. Shapes of baffles after El-Masry and Sarhan (El-Masry and Sarhan, 2000).

To find out how different baffle block shapes affected flow dissipation, an experimental study was carried out on five different baffle block shapes (square, round, equilateral triangle, trapezoidal, and stepped) of downstream weirs. It was found that the square shape has a significant flow-blocking area and a positive impact on flow dissipation (Kang, 2017). Otherwise, Bestawy *et al.* (2013) proved that the concave surface models give low turbulence intensity, change the direction of water, and dissipate energy.

However, vertical semicircular baffles have the most effect on energy dissipation among tested models. A baffle's optimal shape for reducing scour downstream of heading-up structures can vary depending on specific hydraulic conditions and design considerations.

However, based on the research results, it seems that using hollow or semicircular baffles is a well-researched method of minimizing scour downstream of heading-up structures. According to previous research semicircular baffle blocks can be added to already existing heading-up structures to reduce scour downstream of these structures as demonstrated by Abdelhaleem (2013). In addition, the use of hollow semicircular baffles has been studied for scouring and found to be effective in reducing local scour depth downstream of a Fayoum-type weir as illustrated in Fig. 2. With reductions of ~51.86–63.81% for Fr_2 less than 3.5 and 52.5–87.91% for Fr_2 more than 3.5, it decreased the scour length by ~77.06–93.66%. The optimal position of baffles should be in the first third of the floor length, according to Rashed *et al.* (2022). This

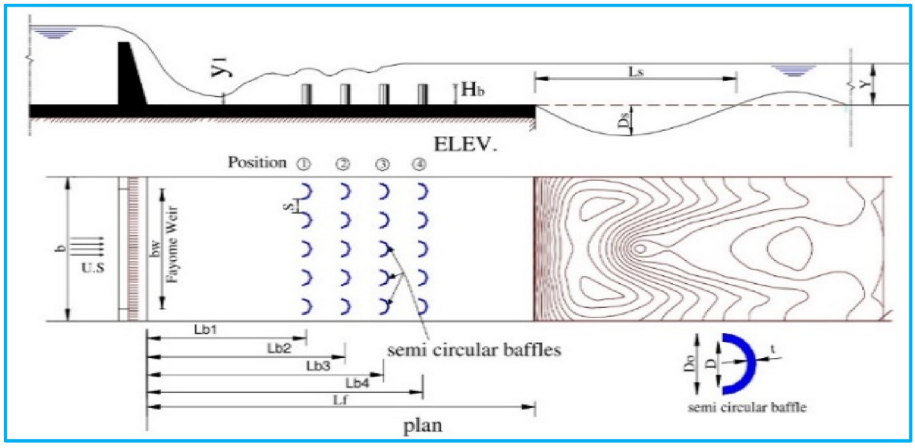

Fig. 2. Arrangement of a single line of baffles block after Abdelhaleem (Abdelhaleem, 2013).

configuration decreases the maximum depth of scour by ~50%. Also, the length of the scour decreased to 31%. Conversely, when the second baffle position is at two-thirds of the floor length, it only reduces the relative scour length to ~57%. All suggested baffle block arrangements, according to a study by Karimi Chahartaghi *et al.* (Karimi Chahartaghi *et al.*, 2022) reduce the maximum scour depth from 52.5 to 77.6% and the maximum scour length from 87.91 to 93.66% and move the maximum scour depth closer to the floor, which might damage the whole structure if the bed downstream of the solid is not scour-protected.

A considerable number of scour depth equations have been developed for a flat floor, downstream of hydraulic structures, encompassing a wide range of experimental parameters. These equations, which establish relationships between scour depth versus flow depth, discharge, and sediment size, are documented in Table 1. Among the early contributors to this field, Wu (1973) studied the scour downstream dam in Taiwan. Dargahi (2003) developed a formula for the scour depth downstream of a spillway.

Based on the analysis of previous research findings, the current study proposes a practical solution to mitigate local scour downstream of hydraulic structures by incorporating perpendicular rasp heads and end sills into the proposed weir. This recommendation stems from the recognition of the detrimental consequences associated with local scour, which often leads to hazardous failures in hydraulic structures.

By using various configurations of rasp heads and end sill heights, this study aimed to effectively reduce the geometrical scour parameters. The suggested system offers a straightforward and feasible approach to enhance the stability and safety of hydraulic structures, as it can be easily implemented as an additional component to the existing heading-up structure.

2. Materials and methods

2.1. Dimensional analysis

The dimensional analysis is used to realize a relationship between the various variables affecting scour parameters. In this research, the maximum scour depth and length are the main studied parameters for the scour hole. The functional relationship for the maximum scour depth and length could be expressed as follows:

$$d_{sm}\ or\ L_{sm} = f\left(H, h, b, Q, V, H_s, y_2, \mathrm{g}, \mu, \rho, d_{50}, \sigma, p_s, L_f, B, t_s, L_s, h_s, L, S, h_b, Wb, L_b\right) \quad (1)$$

where the following parameters are represented in Fig. 3.

2.1.1. Scour hole dimensions

d_{sm} = maximum scour depth (L), L_{sm} = maximum scour length (L).

2.1.2. Flow parameters

H = acting water head above the crest of the weir (L), H_w = head at the rectangular weir in the inlet tank (L), Q = applied discharge along the canal (L^3/T), V = mean velocity of the flow at the downstream cross-section of the flume (L/T), y_2 = tailwater depth (L), μ = dynamic viscosity of the liquid (/ml/T), g = gravity acceleration (L/ T^2), ρ = water density (M/ L^3), H_s = the difference between US. WL, floor bed level, and critical water depth (L), (scour head).

2.1.3. Sediment parameters

d_{50} = the mean particle diameter of sand (L), p_s = density of soil particle (M/ L^3), σ = geometric standard deviation for sediment gradations.

2.1.4. Model and flume parameters

L_f = length of the solid floor (L), B = width of flume and weir (L), h = weir height (L), b = crest width (L), t_s = end sill thickness (L), L_s = end sill length (L), h_s = end sill height (L), h_b = rasp head height (L), W_b = rasp head width (L), L_b = rasp head length (L), L = position of rasp heads from weir (L), S = the distance between rasp heads (L).

In this study, the following parameters are kept constant:

The mean particle diameter of sand ($d_{50} = 0.64mm$), length of the solid floor ($L_f = 1.5$ m),

Table 1. Scour equations downstream of hydraulic structures.

Authors	Year	Formula	Notes
Wu	1973	$\frac{d_{sm}}{H_e} = 2.11\left(\frac{q}{(\mathrm{g}\,H_e^3)^{0.5}}\right)^{0.51}$	Dam in Taiwan
Bijan Dargahi	2003	$\frac{d_{sm}}{H} = 1.7\left(\frac{H}{D_{50}}\right)^{1/4.5}, \frac{L_{sm}}{h_0} = 5\left(\frac{H}{D_{50}}\right)^3$	Spillway

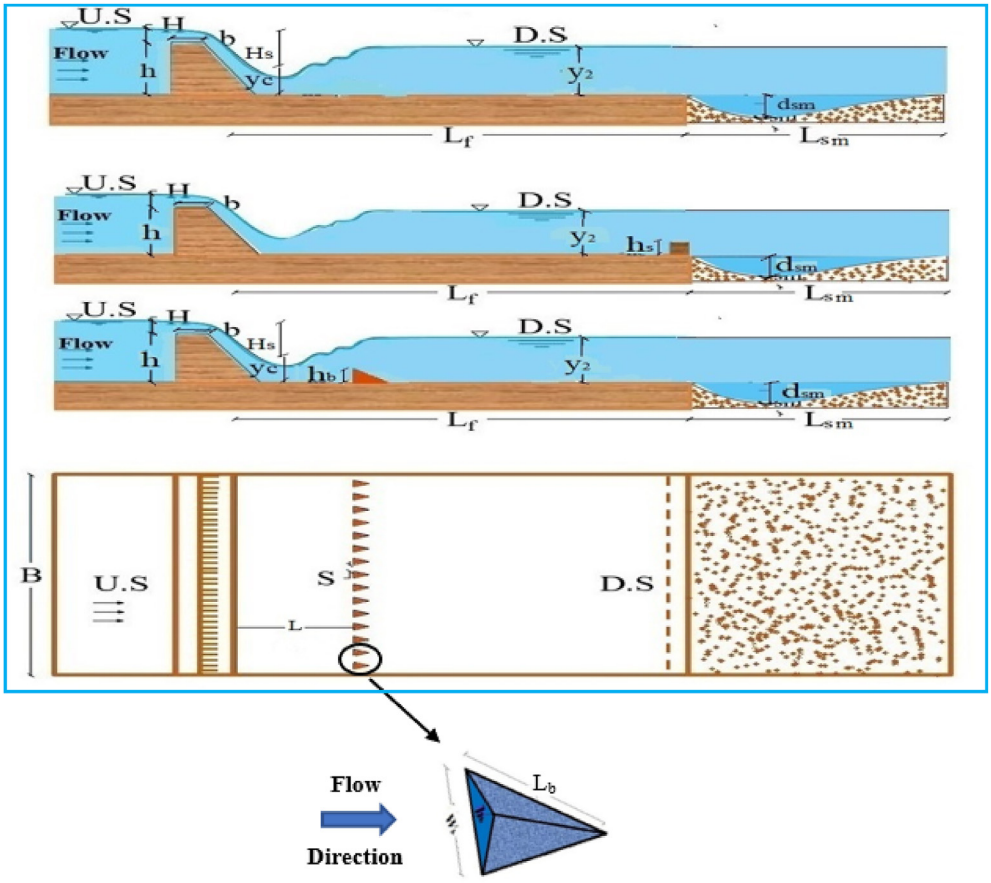

Fig. 3. Layout of Fayoum-type weir with rasp head and end sill.

channel width (B = 0.74 m), end sill thickness ($t_s = 0.025\ m$), water density (ρ = 1000k/ m^3), water viscosity ($\mu = 8.91*\frac{10^{-4}kg}{m.s}$), height of rasp heads (h_b = 0.05 H_s), distance between rasp heads and width (S or $W_b = 3\ h_b = 0.024\ m$), rasp head length ($L_b = 4\ h_b = 0.032m$).

Thus Relation (1) can be simplified to

$$d_{sm}\ or\ L_{sm} = f\left(Q,\ H_s, y_2, L,\ h_s,\ h_b\right) \tag{2}$$

Using the Buckingham dimensional analysis method and assuming no viscous effect and constant relative density, the expressions relating the maximum scour hole dimensions to the essential dependent parameters are as follows:

$$\frac{d_{sm}}{y_2} = f\left(\frac{H_s}{y_2}, \frac{L}{L_f}, \frac{h_s}{H_s}, F_{r2}\right) \tag{3}$$

$$\frac{L_{sm}}{y_2} = f\left(\frac{H_s}{y_2}, \frac{L}{L_f}, \frac{h_s}{H_s}, F_{r2}\right) \tag{4}$$

where $\frac{d_{sm}}{y_2}, \frac{L_{sm}}{y_2}$ = relative maximum scour depth and length to tailwater depth, $\frac{H_s}{y_2}$ = relative scour head to tailwater depth, $\frac{L}{L_f}$ = the relative position of rasp heads to floor length, $\frac{h_s}{H_s}$ = the relative height of the end sill to the scour head, $F_{r2} = \frac{V}{\sqrt{g y_2}}$ = Froude number at the tailwater depth of the flume.

2.2. Experimental setup

Experimental investigations were carried out within a rectangular horizontal flume featuring a recirculation setup, as depicted in Figs. 4 and 5. Experiments were conducted at the laboratory of the Irrigation and Hydraulics Department, Faculty of Engineering, Mansoura University, Egypt. The flume exhibited 6.5 m length, 0.74 m width, and 0.4 m height. The bottom of the flume was constructed using rigid wood covered with galvanized sheets, while the sides of the channel were composed of wooden sheets spanning the length of the channel. To achieve the desired flow rates, three centrifugal

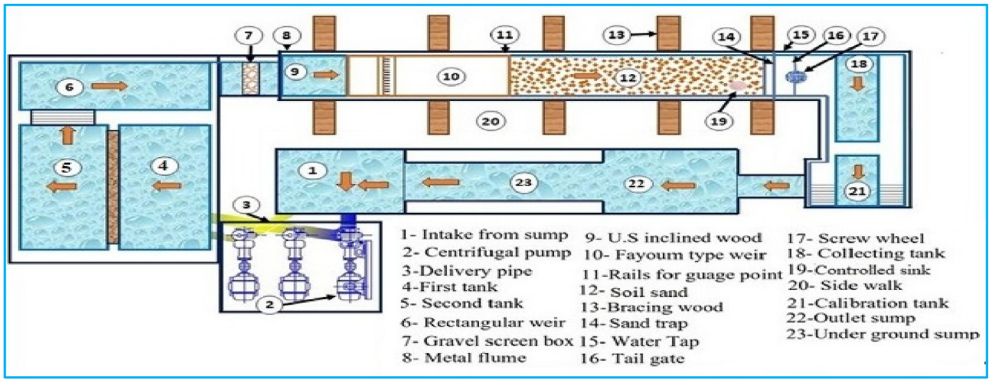

Fig. 4. Schematic of the experimental flume.

Fig. 5. Experimental flume in the laboratory.

pumps were used to lift the specified discharges from an underground tank and deliver them to two inlet tanks through three delivery iron pipes with varying diameters. Furthermore, three inflow control valves were used to ensure precise regulation of the flow rates. One of the two tanks encompassed a calibrated rectangular weir, enabling accurate measurement of the applied flow discharge rate.

Subsequently, the mean flow velocity was computed using the widely used discharge equation ($Q = \frac{2}{3}\, c_d\, B\, \sqrt{2\,g}\, H^{3/2}$). The tailwater depth can be adjusted by a tailgate installed at the end of the flume. Also, there is a point gauge in the flume used to measure bed elevations and this device had a vertical scale with an accuracy of 0.1 mm for measuring scouring sediment and water table depths. This point gauge was installed on a carriage to slide in the transverse and longitudinal directions. The model of a Fayoum-type weir with a solid floor placed within 2 m of flume length. A 4.0-m-long partition filled with nonuniform sand with a thickness of 0.20 m.

2.3. Experimental models

A Fayoum-type weir, constructed using high-quality Sweden wood, served as the heading-up structure in conducted experiments. The weir exhibited specific dimensions, including a crest length of 0.74 m, height of 0.12 m, and a slope ratio of 1 : 2. The structure featured a solid floor, also made of Sweden wood, with a length of 2.0 m and a width of 0.74 m. The weir's location occurred at a distance of 0.33 times the length of the solid floor. To facilitate energy dissipation, wooden end sills were used, with four heights used in the setup. The heights of these end sills were set at specific ratios relative to H_s, (0.05 H_s, 0.1 H_s, 0.15 H_s, and 0.2 H_s). End sills remained constant in thickness (0.025 m) with the full width of the channel throughout experimental runs. In addition, precast aluminum rasp heads were strategically positioned at locations corresponding to one-third, two-thirds, and the entire length of the solid floor. These rasp heads had a uniform height of 0.05 H_s, as visually illustrated in Figs. 3 and 6.

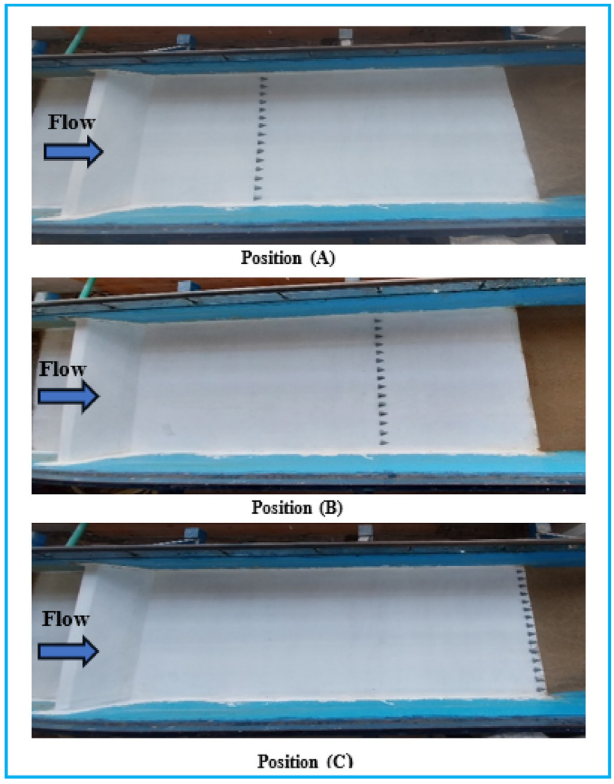

Fig. 6. Fayoum-type weir with rasp heads in the laboratory.

2.4. Equilibrium time

All experiments were conducted for 4 h to ensure the attainment of equilibrium scour conditions. Scour depth results were obtained for the case of a flat floor without sills and rasp head under the given hydraulic conditions of $Fr_2 = 0.39$, $Q = 24.17$ l/s, and $y_2 = 9$ cm. The temporal variation of scour depth was plotted on a graph, as shown in Fig. 7, to illustrate the relationship with time. The scour depth exhibited significant changes, with a rapid initial rise. Within the first 15 min of operation, 58% of the equilibrium scour depth was reached. Subsequently, the scour depth continued to increase and surpassed 80% within 60 min. A stabilizing stage was then reached during the subsequent hour, resulting in a notable reduction in scour rate. At around 120 min, the scour depth reached 94%, and after ~165 min, it had reached 98% of the equilibrium value. Over the remaining 75 min, spanning a total of 240 min (4 h), the scour hole remained relatively unchanged, with an insignificant increase in the maximum scour depth of less than 2%. Rashed *et al.* (2022) reported that, after 120 min, there was no discernible movement of sediment particles within the scour hole. These findings highlight the substantial contribution of baffles in reducing the scour depth, as the ordinary case without baffles yielded most of the observed scour depth.

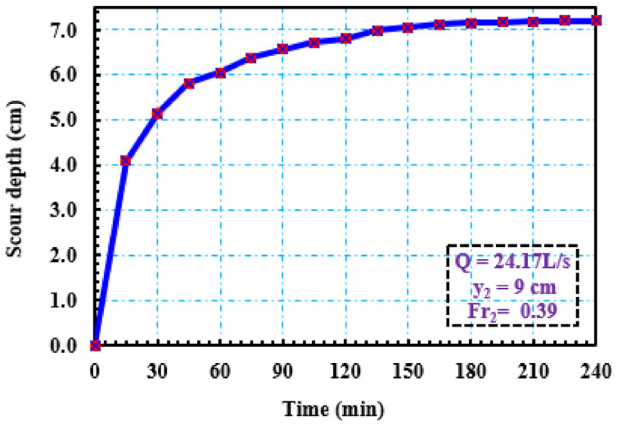

Fig. 7. Developing scour depth versus time for clear water local scour for a flat floor.

2.5. Sediment characterizations

The bed material selected for the experiments was sand, which possessed specific dimensions downstream of a Fayoum-type weir. The sand layer had a thickness of 20 cm, a width of 0.74 cm, and extended for a length of 4.5 m. In terms of particle size distribution, the sand exhibited a geometric standard deviation ratio (σ_g) of 1.7, indicating a nonuniform sediment composition. To assess the uniformity of the sediment, the standard geometric deviation is used, with values exceeding 1.3 signifying nonuniformity. In the present case, with $\sigma_g = 1.7$, the bed material was characterized as nonuniform. Consequently, armoring phenomena were expected to

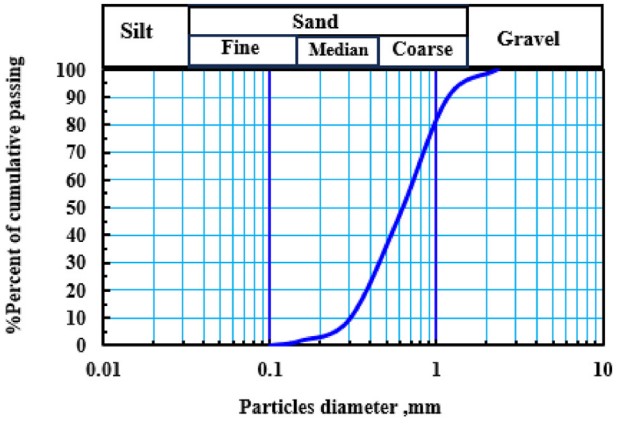

Fig. 8. Sieve analysis of bed material.

Table 2. Sediment material characterization.

Bed material	$d_{15.9}$	d_{30}	d_{50}	d_{60}	$d_{84.1}$	σ_g	SG
Sand	0.35	0.46	0.64	0.77	1.10	1.76	2.65

occur both within the scour hole and along the channel bed. Comprehensive information regarding the particle size distribution of the sand can be observed in Fig. 8 and Table 2, which illustrates the results of the sieve analysis.

2.6. Hydraulic conditions

The ratio of flow intensity denoted as V/V_a holds significant importance in assessing scouring processes involving nonuniform sediments. Here, V_a represents the critical velocity at which the transition occurs from clear-water conditions to live-bed conditions in a flow that carries sediment. In the case of uniform sediments, V_a corresponds to V_c. When V/V_a exceeds 1, live-bed conditions prevail in the progress, ultimately reaching clear-water conditions, as depicted in Table 3. Melville and Sutherland (1988) propose a formula for estimating V_a, which yields $V_a = 0.8V_{ca}$. Here, V_{ca} represents the mean flow velocity at which armoring of a nonuniform sediment bed becomes impossible. In situations where there is no upstream sediment resupply, this condition signifies the emergence of the most stable and armored bed for a given bed material. The critical velocities V_{ca} and V_c can be determined using the logarithmic form of the velocity profile:

$$\frac{V_{Ca}}{u_{*Ca}} = 5.75 \log\left(\frac{5.73\, y}{D_{50a}}\right) \tag{5}$$

$$u_{*ca} = 0.0115 + 0.012\, d^{1.4} \tag{6}$$

$$0.1\ \text{mm} < d < 1\text{mm}$$

where u_{*ca} is the critical shear velocity for the median armor size,

$$D_{50a} = \frac{D_{max}}{1.8} \tag{7}$$

D_{max} = maximum particle size and is determined from the particle size distribution.

From Fig. 8 and Table 2

$d_{50} = 0.64$ mm

$D_{max} = 2.5$

$D_{50a} = 1.39$

$d_{84.1} = 1.10$ and $d_{15.9} = 0.35$

$$\sigma g = \sqrt{d_{84,1}/d_{15.9}} \tag{8}$$

$\sigma g = 0.65$

V2/Vca<1 is a clear water condition as shown in Table 3.

2.7. Experimental scheme

In this research, the experimental work was classified into three cases. Each of the experimental cases was restricted to the same flow conditions:

(1) Three flow discharge rates equal to 24.17, 20.63, and 17.29 l/s.
(2) Twelve Froude numbers (F_{r_2}) are used as follows:
(0.19, 0.20, 0.22, 0.23, 0.24, 0.26, 0.27, 0.28, 0.29, 0.31, 0.33, and 0.39).

Table 3. Hydraulic conditions for all experiments.

Variables	H_w	y_2	V_2	Fr_2	u*c	V_{ca}	$Va = 0.8\,V_{ca}$	V_2/V_{ca}
	cm	cm	m/s		m/s	m/s	m/s	
Discharge (Lit/s)		11.50	0.20	0.19		0.46	0.37	0.55
		11.00	0.21	0.20		0.46	0.37	0.58
17.29	8.00	10.50	0.22	0.22	0.03	0.46	0.36	0.61
		10.00	0.23	0.24		0.45	0.36	0.65
		9.00	0.26	0.28		0.44	0.36	0.73
		11.50	0.24	0.23		0.46	0.37	0.66
20.63	9.00	10.50	0.27	0.26	0.03	0.46	0.36	0.73
		9.00	0.31	0.33		0.44	0.36	0.87
		11.50	0.28	0.27		0.46	0.37	0.77
		11.00	0.30	0.29		0.46	0.37	0.81
24.17	10.00	10.50	0.31	0.31	0.03	0.46	0.36	0.85
		9.00	0.36	0.39		0.44	0.36	1.00

(3) Tail water depths (y_2) are adjusted by a tailgate as follows (9.00, 10.00, 10.50, 11.00, and 11.50 cm).

The three experimental sets are the following:

(1) Flat floor without any sills or rasp heads to be used as a reference to the results of experiments of end sill and rasp heads as shown in Fig. 3.
(2) Four relative heights of the end sill are used as follows:

$$h_s = (0.05, 0.1, 0.15, \text{and } 0.2)\, H_s$$

(3) Rasp head blocks with one height and three arrangements on the floor as in Figs. 3 and 6.

where

$$h_b = 0.05H_s, L = 0.33L_f,$$

$$L = 0.67L_f,$$

$$L = 1.0\, L_f$$

h_b = constant = equivalent height to the most effective height of the end sill.

3. Results and discussion

The present study used dimensional analysis theory to investigate the influence of an equivalent height of the rasp head to the most effective height of the end sill that reduces scour parameters. The nondimensional variables influence the maximum scour depth and length, considering different heights of the end sill and arrangements of rasp heads are studied. The results of the tested experiments are listed in Tables 4 and 5.

To establish empirical relationships between these variables, the statistical software SPSS 27 was used. In addition, the Surfer program was used to generate a 3D model and a bed profile of the sedimentary bed, enabling visualization of the scour area downstream of the Fayoum-type weir. By using this software, a comprehensive representation of the topography and characteristics of the scour region can be depicted, allowing for a better understanding and analysis of the scour phenomenon.

Table 4. Experimental results for relative scour depth (d_{sm}/ y_2) of the tested cases.

dsm/y_2	Flat floor	Flat floor with end sill				Flat floor with rasp heads		
						$h_b = 0.05H_s$		
F_{r_2}	F. F	$h_s = 0.05H_s$	$h_s = 0.1H_s$	$h_s = 0.15H_s$	$h_s = 0.2H_s$	$L = 0.33L_f$	$L = 0.67L_f$	$L = L_f$
0.19	0.122	0.030	0.039	0.096	0.140	0.004	0.017	0.027
0.20	0.220	0.037	0.047	0.115	0.148	0.007	0.020	0.039
0.22	0.276	0.052	0.067	0.158	0.194	0.010	0.033	0.049
0.23	0.235	0.043	0.078	0.116	0.183	0.014	0.050	0.072
0.24	0.319	0.060	0.090	0.181	0.240	0.007	0.054	0.059
0.26	0.295	0.077	0.112	0.226	0.248	0.060	0.069	0.071
0.27	0.270	0.119	0.139	0.232	0.261	0.063	0.074	0.067
0.28	0.364	0.090	0.158	0.289	0.297	0.083	0.084	0.089
0.29	0.291	0.127	0.191	0.261	0.278	0.086	0.103	0.096
0.31	0.350	0.144	0.221	0.324	0.307	0.133	0.137	0.141
0.33	0.557	0.322	0.331	0.389	0.356	0.246	0.222	0.233
0.39	0.800	0.500	0.500	0.580	0.489	0.358	0.478	0.340

Table 5. Eperimental results for relative scour length, (L_{sm}/ y_2) of the tested cases.

Lsm/y_2	Flat floor	Flat floor with end sill				Flat floor with rasp heads		
						$h_b = 0.05H_s$		
F_{r_2}	F. F	$h_s = 0.05H_s$	$h_s = 0.1H_s$	$h_s = 0.15H_s$	$h_s = 0.2H_s$	$L = 0.33L_f$	$L = 0.67L_f$	$L = L_f$
0.19	2.43	1.39	1.57	2.43	3.30	0.35	0.17	0.52
0.20	2.55	1.45	1.64	2.73	3.64	0.36	0.36	0.55
0.22	2.86	1.71	1.90	3.62	4.38	0.52	0.70	0.76
0.23	2.96	1.91	2.09	2.96	4.17	0.57	0.76	1.22
0.24	3.80	2.20	2.40	4.00	5.40	0.80	1.74	1.40
0.26	3.62	2.48	2.86	4.57	6.10	0.95	1.90	1.71
0.27	3.83	2.96	2.96	4.52	5.39	1.39	2.00	1.74
0.28	5.11	2.89	3.78	6.00	8.44	1.78	2.67	2.00
0.29	4.00	3.64	3.82	4.91	8.00	2.00	2.36	2.22
0.31	6.29	5.52	4.57	5.90	9.14	2.67	2.73	3.81
0.33	8.00	7.11	6.89	9.11	11.33	4.44	3.33	5.33
0.39	12.89	12.44	10.67	11.56	15.11	6.22	7.78	6.67

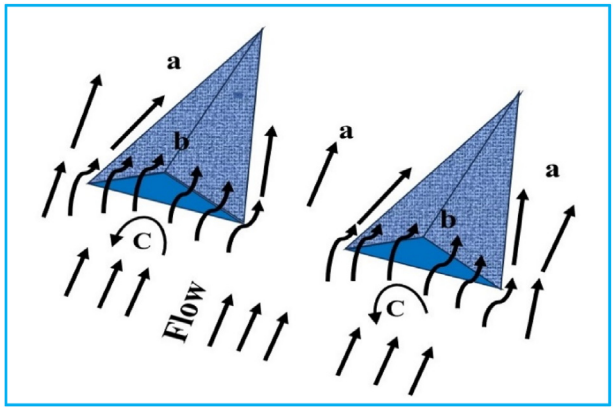

Fig. 9. Observed types of flow across rasp heads.

During the experimental work, the analysis allowed for the identification of three distinct types of flow across the row of rasp heads as depicted in Fig. 9.

These flow patterns can be categorized as follows:

(1) Diverted flow

This type of flow occurs when water passes between the rasp heads, resulting in a diversion of the flow path.

(2) Overtopping flow

In this case, the flow passes over the rasp heads, leading to a flow pattern characterized by water flowing above the baffles.

(3) Eddy current

This flow pattern exhibits a curved flow path, generating vortices in front of the heads due to the curvature of the flow.

These observations provide valuable insights into the dynamics of flow around the rasp heads and contribute to a better understanding of the mechanisms that play in the scour process downstream of the Fayoum-type weir. The main flow characteristic observed was the rapid formation of a hydraulic jump from the initial supercritical condition, resulting in the generation of large secondary flows and clockwise vortices. These secondary flows were instrumental in the development of multiple scour holes downstream of the weir. Also, the number of scour holes formed was influenced by the type of bed material, discharge factor, and Froude number, highlighting their role in determining the quantity of holes generated.

3.1. Effect of downstream Froude number on scour hole dimensions for the case of flat floor

Froude number, F_{r2} is a significant factor influencing the scour hole's characteristics (scour depth and length). Results indicated a direct relationship between the relative depth and length of the scour hole to the height of the tailwater ($\frac{d_{sm}}{y_2}$ and $\frac{L_{sm}}{y_2}$) with Froude number F_{r2}. When the Froude number increases the flow velocity increases, the shear force acting on sediment particles exceeds the resisting forces (like particle weight or cohesion), and it can lead to scouring, which is the erosion or removal of sediment from the bed of the river as illustrated in Figs. 10 and 11. In these figures, the scour hole dimensions were measured in the case of a flat floor to use as a reference to investigate the effect of end sill and rasp heads under the same flow conditions on scour hole dimensions.

3.2. Effect of relative height of end sill on scour hole dimensions compared with a flat floor

3.2.1. Effect of relative height of end sill on scour depth

The relationship between the maximum relative scour depth to tailwater depth (d_{sm}/y_2) is depicted in Fig. 12, along downstream Froude numbers F_{r2},

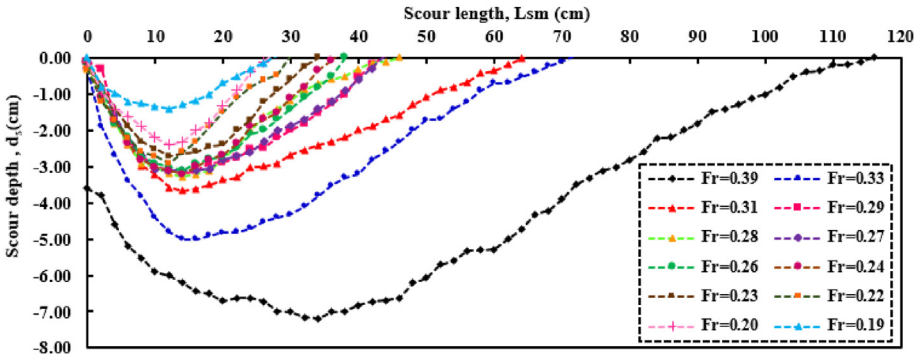

Fig. 10. Scour hole profile for the case of a flat floor (FF).

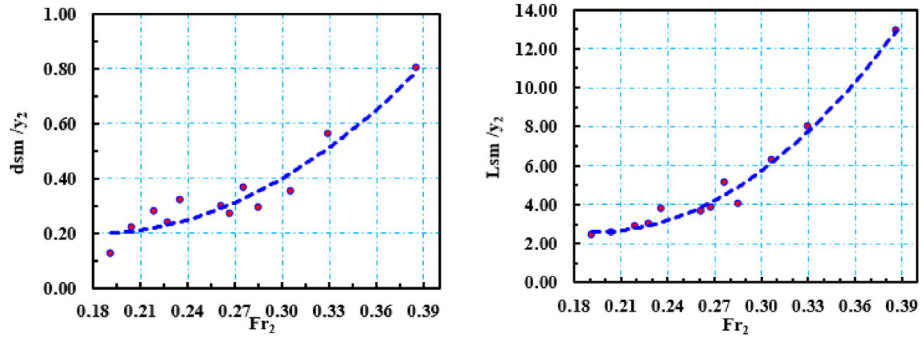

Fig. 11. Maximum relative scour depth and length versus Froude number for a flat floor (FF).

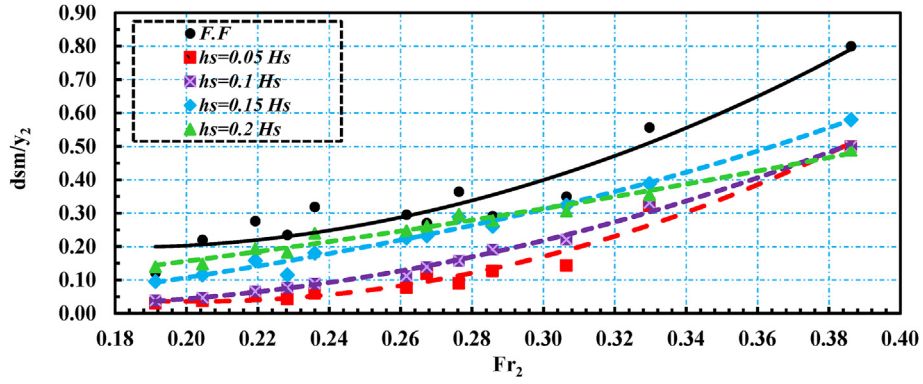

Fig. 12. Relative scour depth versus Froude number for relative heights of end sill (ES).

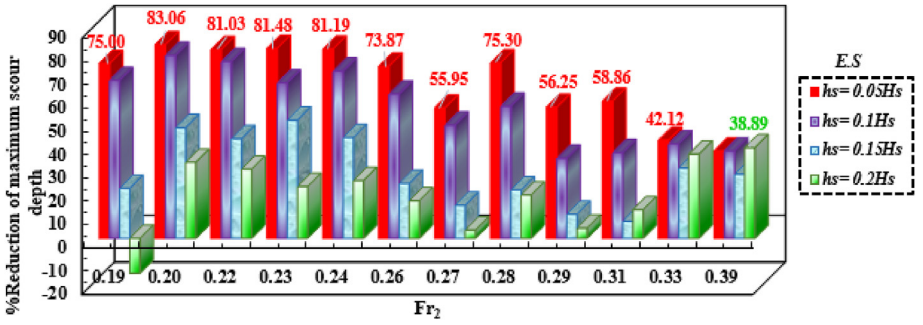

Fig. 13. Reduction percentage in the relative maximum scour depth for relative heights of end sill (ES).

ranging from 0.19 to 0.39. The graph shows the experimental results for four different relative heights of the end sill, providing a comparative analysis with a flat floor configuration.

From the figure, it can be concluded that:

(1) For all experimental runs, the relative depth of scour hole, (d_{sm}/y_2) increases with increasing the downstream Froude number.

(2) For most flow conditions, all relative heights of the end sill led to a reduction in maximum scour depth compared with a flat floor with no sills, the only exception occurs at $F_{r2} = 0.19$, where the end sill height ($h_s = 0.2\ H_s$) causes a 15% increase in scour depth compared with a flat floor.

(3) The most efficient height for the end sill, resulting in the maximum reduction in scour depth, was found to be $h_s = 0.05\ H_s$. This height led to a reduction nearly from 37.5 to 83% at all tested downstream Froude numbers compared with a flat floor without an end sill. However, it is noteworthy that at $F_{r2} = 0.39$, the end sill's height ($h_s = 0.2\ H_s$) achieved the most significant reduction in scour depth with 38.89% as illustrated in Fig. 13.

3.2.2. *Effect of the relative height of end sill on scour length*

The relationship between the downstream Froude numbers, F_{r2}, which ranged from 0.19 to 0.39 for the

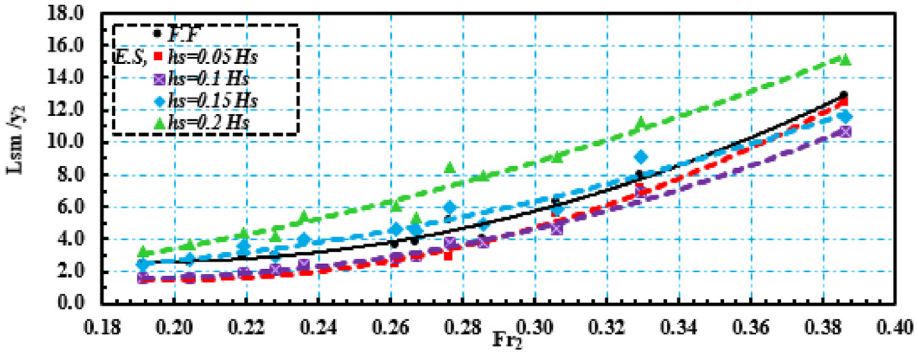

Fig. 14. Relative scour length versus Froude number for relative heights of end sill (ES).

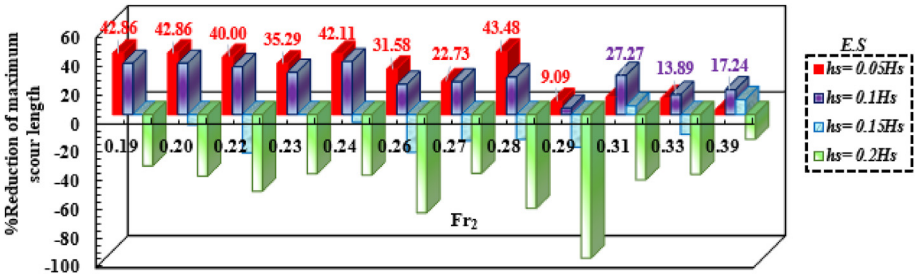

Fig. 15. Reduction percentage in the maximum scour length for relative heights of end sill (ES).

relative heights of the end sill, and the maximum relative scour length, (L_{sm}/y_2), is depicted in Fig. 14, where the experimental results are plotted relative to a flat floor without end sill.

From the figure, it can be concluded that:

(1) For all the experimental runs, the relative scour length (L_{sm}/y_2) increases with increasing the downstream Froude number.
(2) Two end sill heights, h_s =(0.05, and 0.1)H_s, effectively minimize the maximum scour length across all flow conditions when compared with a flat floor. Conversely, two alternative end sill heights, h_s = (0.15, and 0.2)H_s, led to an increase in the maximum scour length compared with a flat floor.
(3) For $F_{r2} \leq 0.29$, the effective end sill height for reducing scour length is $h_s = 0.05\ H_s$, resulting in a scour length reduction ranging from 9.09 to 43.48%. Otherwise, when $F_{r2} > 0.29$, the end sill's height, $h_s = 0.1\ H_s$, led to a scour length reduction of nearly 13.98–27.27 %, as depicted in Fig. 15.

3.3. Effect of rasp head on scour hole dimensions

3.3.1. Effect of rasp head with an equivalent relative height of end sill on scour depth

The relationship between the maximum relative scour depth and downstream Froude number is illustrated in Fig. 16. The values of Froude number, F_{r2}, ranged from 0.19 to 0.39. The equivalent height of rasp heads is studied at three different positions along the downstream floor length. The most effective height of the end sill that reduces scour depth is considered with the flat floor as a comparative study.

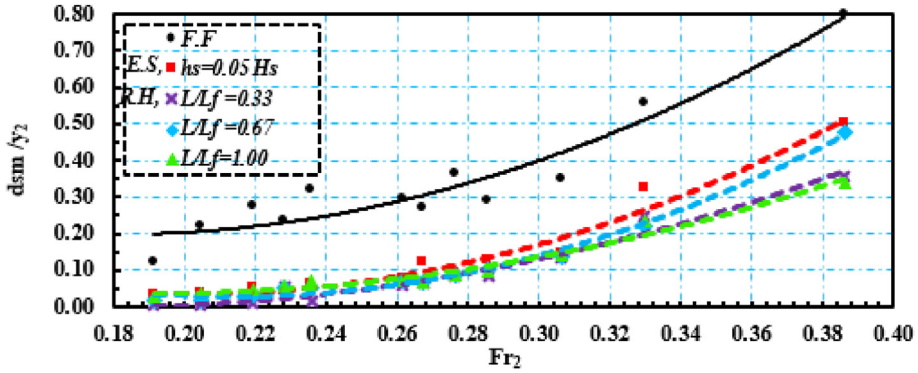

Fig. 16. Maximum relative scour depth (d_{sm}/y_2) versus Froude numbers for three arrangements of rasp heads (RH).

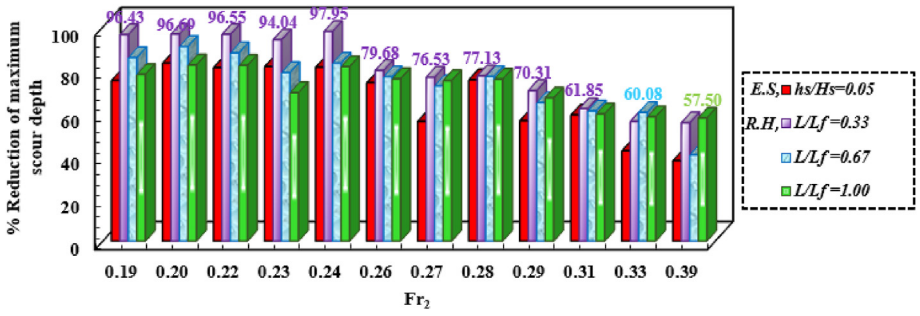

Fig. 17. Reduction percentage in the relative maximum scour depth for three arrangements of rasp heads (RH).

From the figure, it can be concluded that:

(1) For all the conducted experimental runs, the relative scour depth (d_{sm}/y_2) increases with increasing downstream Froude number.
(2) All energy dissipators reduce maximum scour depth for all flow conditions compared with the flat floor with no sills and no rasp heads.
(3) The rasp heads with an equivalent relative height of the most efficient height of the end sill situated at one-third of the downstream floor length, L/ L_f = 0.33 are more effective than end sill in minimizing scour depth. They give a reduction in scour depth with nearly 61.85–96.43% at all suggested values of the Froude number except at F_{r2} = 0.33 *to* 0.39.
(4) The rasp heads positioned at two-thirds of the floor length with F_{r2} = 0.33 achieve a scour depth reduction of ~60%. In addition, when the rasp heads are located at the end of the floor at F_{r2} = 0.39, there is a scour depth reduction of ~57.5% as illustrated in Fig. 17.

3.3.2. Effect of rasp heads with an equivalent relative height of end sill on scour length

The association between 12 downstream Froude values, $F_{r2,}$ ranging from 0.19 to 0.39, for three different arrangements of rasp heads and the maximum relative scour length, L_{sm}/y_2 is illustrated as shown in Fig. 18. An equivalent relative height of the best relative height of the end sill that reduc-esreduces scour length is considered. Experimental results are plotted and explained compared with a flat floor with no sills and no rasp heads.

According to Fig. 18

(1) All the arrangements of rasp heads minimize scour length for all considered flow conditions.
(2) A single line of rasp head is used at one-third of the downstream floor length, giving the maximum reduction in scour length at all values of Froude number compared with the flat floor, and end sill with the same relative height, and other arrangements of rasp heads.
(3) This reduction in scour length ranges from 50 to 85.7% except at F_{r2} = 0.33 and 0.19. The single line of rasp heads is located at two-thirds of the floor length giving the maximum reduction in scour length with nearby 58.33 and 92.84%, respectively, as shown in Fig. 19.

3.4. Longitudinal scour hole sections and profiles of some tested cases

To obtain and represent scour depth readings, the measurement gap was marked every 2 cm at the

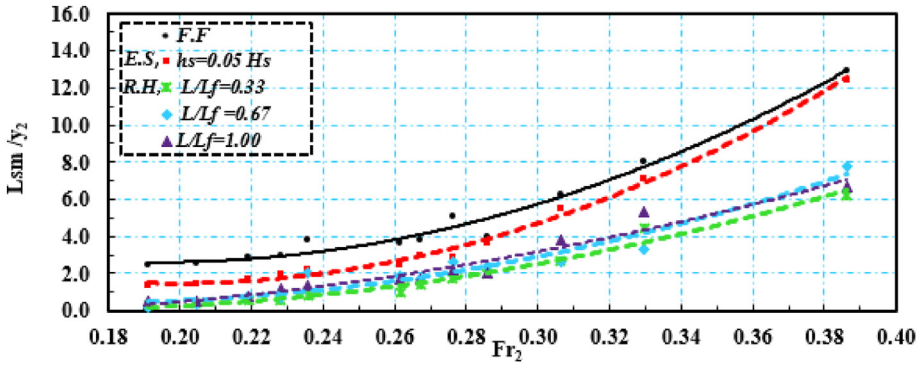

Fig. 18. Maximum relative scour length, L_{sm}/y_2 versus Froude numbers for three arrangements of rasp heads (RH).

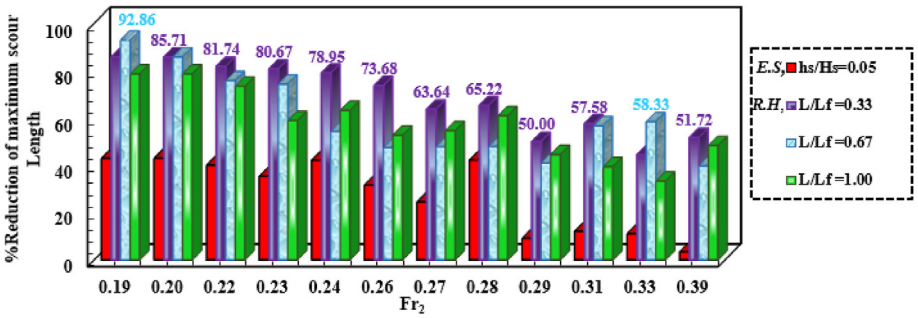

Fig. 19. Reduction percentage in the maximum scour length for three arrangements of rasp heads (RH).

flume's centerline in the direction of the X-axis.- Moreover, it was measured every 5 cm along the X and Y axes to represent the contour maps topographies and three-dimensional models created by the Surfer software. Figs. 20 and 21 illustrate the recorded actual scour hole profiles for the optimal cases of rasp head arrangements and heights of end sill compared with a flat floor at the largest two values of the Froude number.

4. Derivation of maximum scour parameters

To capture the essential factors influencing the design process, it is imperative to formulate mathematical formulae that express these parameters. Specifically, relations (3) and (4) incorporate dimensionless parameters, namely (d_{sm}/ y_2) and (L_{sm} / y_2), which serve as key variables in establishing a nonlinear regression equation in conjunction

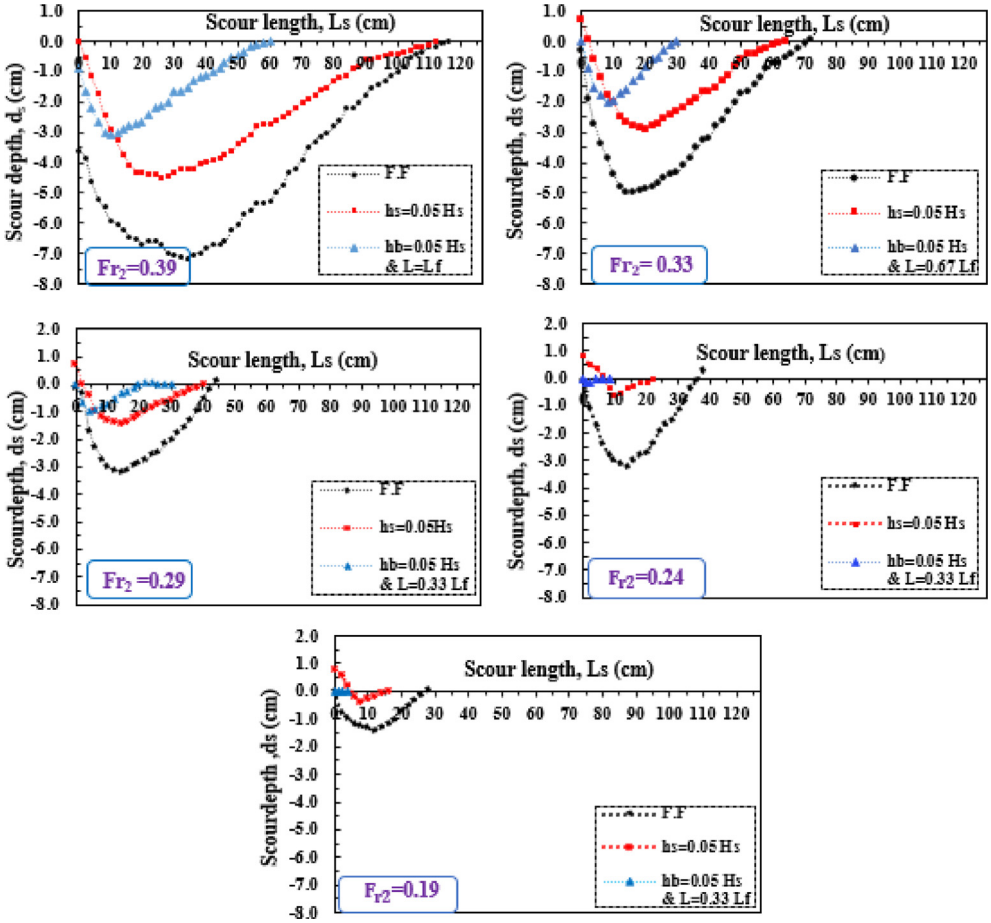

Fig. 20. Scour hole profile at the flume center for a flat floor, end sill, $h_s = 0.05H_s$, and rasp heads, $h_b = 0.05H_s$ at $F_{r2} = 0.19, 0.24, 0.29, 0.33,$ and 0.39.

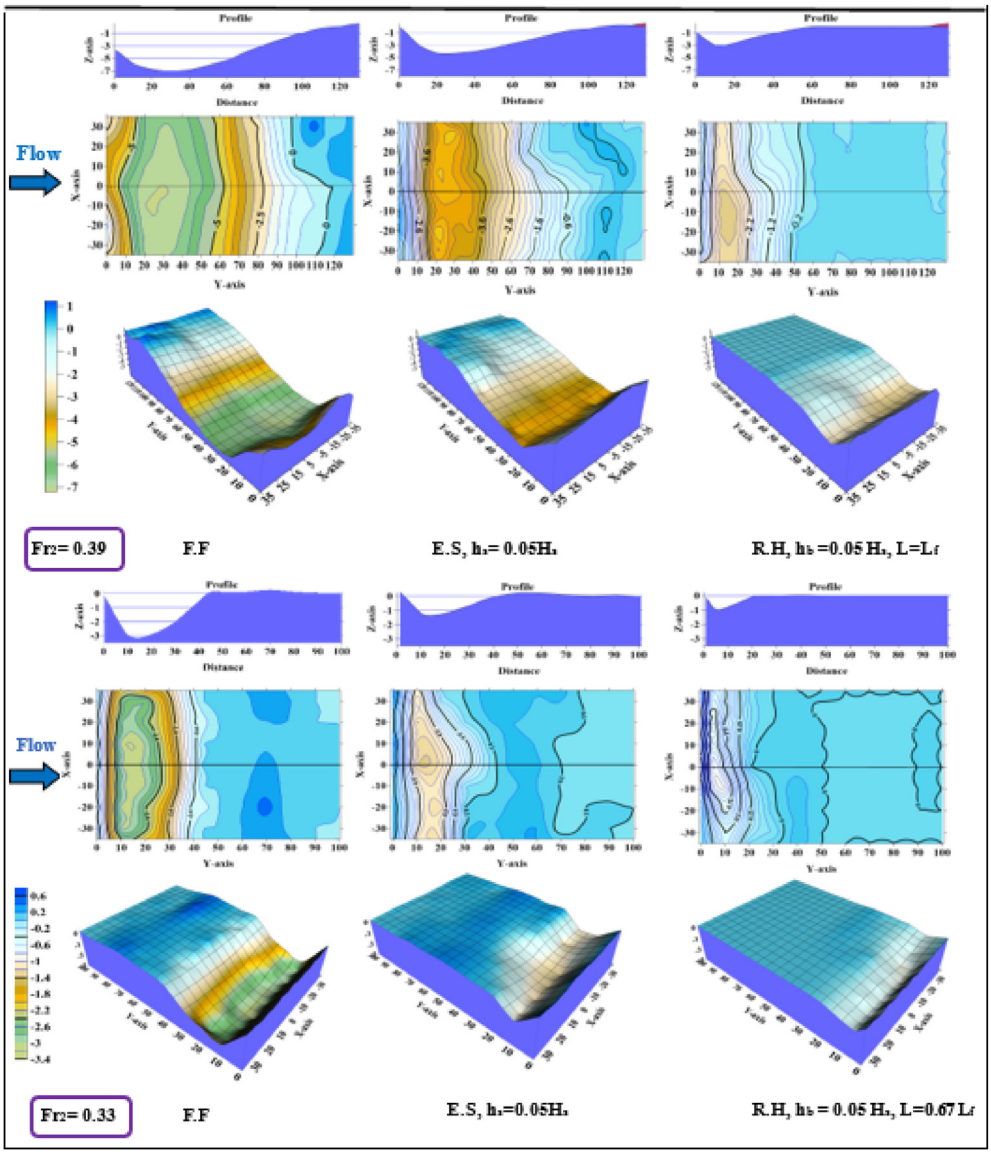

Fig. 21. Scour profile for a flat floor, end sill, $h_s = 0.05H_s$, and rasp heads, $h_b = 0.05H_s$ at $L = L_f$ for $F_{r2} = 0.39$, and $L = 0.67\ L_f$ for $F_{r2} = 0.33$.

with other dimensionless parameters. It is important to acknowledge that the relationships are restricted to the experimental data used within the scope of the present study.

To determine the most accurate nonlinear regression equations, the Social Science Statistical Package (SPSS) is used. The objective is to minimize the errors between the measured and predicted values. As the coefficient of determination approaches unity, the predicted outcomes align closely with the measured results, indicating the effectiveness of the derived relationships. During the analysis of experimental outcomes, various forms of relationships are proposed, with different initial values assigned to unidentified coefficients. This approach allows for the identification of the most optimal coefficients that yield the best achievable results.

The following relations are derived to represent the diverse heights of end sills and positions of rasp heads investigated within the framework of this research. Using the suggested values for variables (F_{r2}, $H_s/\ y_2$, $h_s/\ H_s$, $L/\ L_f$) and the relations variables ($d_{sm}/\ y_2$) and ($L_{sm}\ /\ y_2$), we can predict the values for the following relationships under conditions as shown in Table 6.

- Case of the flat floor

$$\frac{d_{sm}}{y_2} = 53.799\ (F_{r2})^{4.958} + 0.071\left(\frac{H_s}{y_2}\right)^{2.407} \tag{9}$$

$$\frac{L_{sm}}{y_2}=739.877\,(F_{r2})^{4.543}+0.89\left(\frac{H_s}{y_2}\right)^{2.012} \quad (10)$$

- Case of the flat floor with various heights of end sills

$$\frac{d_{sm}}{y_2}=8.710\,(F_{r2})^{3.060}-0.181\left(\frac{H_s}{y_2}\right)^{-0.94}+0.74\left(\frac{h_s}{H_s}\right)^{0.773} \quad (11)$$

$$\frac{L_{sm}}{y_2}=285.692\,(F_{r2})^{3.502}+0.002\left(\frac{H_s}{y_2}\right)^{10.52}+651.554\left(\frac{h_s}{H_s}\right)^{3.270} \quad (12)$$

- Case of the flat floor with rasp heads

$$\frac{d_{sm}}{y_2}=24\,(F_{r2})^{4.30}-0.01\left(\frac{H_s}{y_2}\right)^{0.611}+0.018\left(\frac{L}{L_f}\right)^{1.136} \quad (13)$$

$$\frac{L_{sm}}{y_2}=198\,(F_{r2})^{3.486}-0.48\left(\frac{H_s}{y_2}\right)^{-0.199}+0.47\left(\frac{L}{L_f}\right)^{1.84} \quad (14)$$

Fig. 22 demonstrates the correlation between the experimentally measured relative maximum scour parameters ($d_{sm}/\ y_2$), ($L_{sm}\ /\ y_2$), and the calculated values obtained from Relations (9) and (10) for the case of a flat floor. The coefficients of determination for these relationships are 0.97 and 0.99. Fig. 23 displays the correlation between the experimentally measured relative maximum scour parameters ($d_{sm}/\ y_2$), ($L_{sm}\ /\ y_2$), and the calculated values for the floor with end sill using relations (11) and (12), with coefficients of determination 0.95 and 0.965. Furthermore, Fig. 24 illustrates the correlation between the experimentally measured relative maximum scour parameters ($d_{sm}/\ y_2$), ($L_{sm}\ /\ y_2$), and the calculated values obtained from relations (13) and (14) for flat floor with rasp heads. The coefficients of determination for these relationships are 0.95 and 0.949.

Table 6. Limitations for derived empirical equation parameters.

Case	Parameters					
	Fr_2	y_2	H_s	h_s	L_f	L
Flat floor	0.19–0.39	9.00–11.50 cm	16.68–16.83 cm		1.50 m	
End sill	0.19–0.39	9.00–11.50 cm	16.68–16.83 cm	0.80–3.40 cm	1.50 m	
Rasp heads	0.19–0.39	9.00–11.50 cm	16.68–16.83 cm		1.50 m	0.50–1.50 m

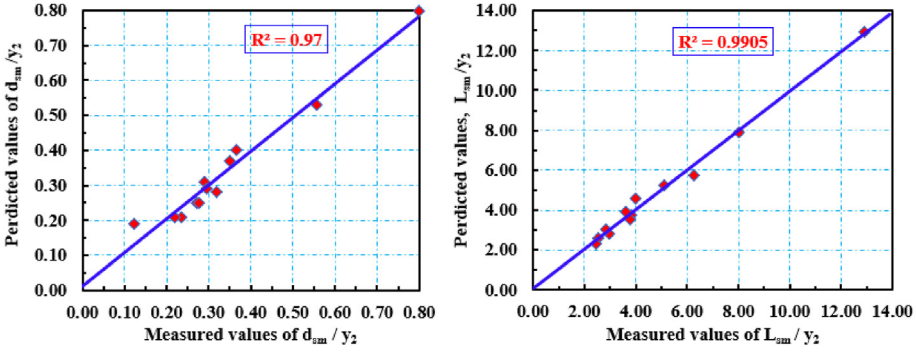

Fig. 22. Measured values, d_{sm}/y_2 and L_{sm}/y_2 versus predicted values for a flat floor.

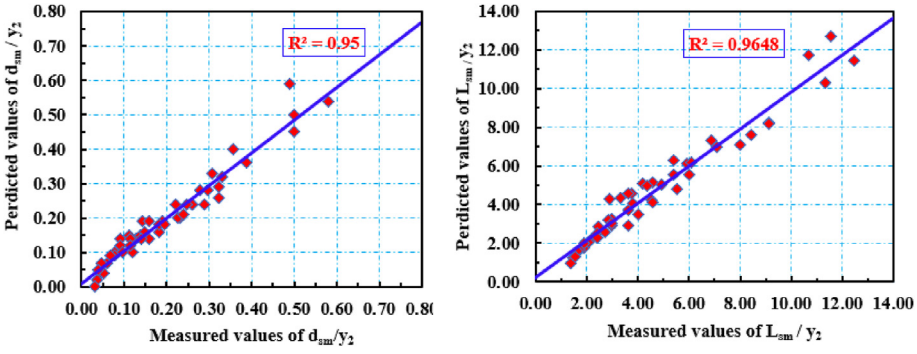

Fig. 23. Measured values of d_{sm}/y_2 and L_{sm}/y_2 versus predicted values for the floor with the end sill.

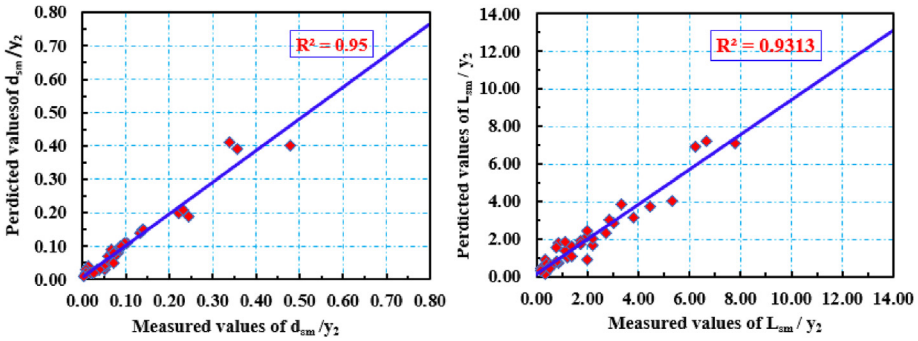

Fig. 24. Measured values of (d_{sm}/y_2 and L_{sm}/y_2) versus predicted values for rasp heads in three positions.

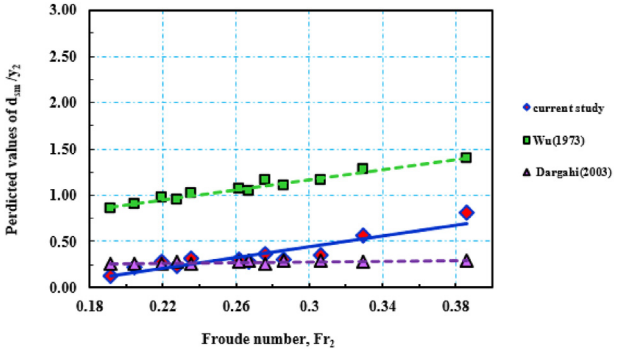

Fig. 25. Comparison between the measured and predicted values of relative scour depth from other studies.

5. Calibration of experimental measurements

The experimental results for flat floors and previous studies from each of Wu (1973), and Dargahi (2003) are illustrated in Fig. 25. Empirical equations of Dargahi (2003) generate extremely similar values of relative scour depth ($d_{sm}/\ y_2$) obtained from the current study. However, Wu (1973) generates higher values of relative scour depth than other equations. This might be due to the d_{90} particle size variation. The equation in Dargahi (2003) which is illustrated in Fig. 25 provided an acceptable estimation for a measured scour depth compared with the equations collected from the review, and then the experimental data for flat floors are acceptable. H_e is the elevation difference between upstream and downstream water levels, D_{90} = particle size of which 90% of the material is finer.

6. Conclusions

The experimental investigation and statistical analysis conducted on local scour downstream of a Fayoum-type weir, considering the implementation of different energy dissipators such as end sills with varying relative heights and rasp heads with an equivalent height to the most effective relative height of the end sill, have yielded the following key findings and conclusions:

(1) Dimensions of the scour hole increase significantly as the downstream Froude number rises.
(2) All energy dissipators used in the experimental study effectively reduced the maximum relative scour parameters downstream of the Fayoum-type weir compared with the flat floor.
(3) The end sill and rasp heads can serve as additional components to mitigate scour dimensions downstream of the Fayoum-type weir.
(4) Using four relative heights of the end sill on the downstream floor causes a reduction in maximum relative scour depth ranging from 37.5 to 83.0%. However, using only two relative heights of the end sill reduces maximum relative scour length by 9–43.38% for Froude numbers below 0.29 and from 13.9 to 27.27% for Froude numbers above 0.29.
(5) Implementing rasp heads with an equivalent height to the most effective relative height of the end sill results in a significant reduction in both relative scour depth and length, ranging from 61.85 to 96.43% and 50–85.7%, respectively, when positioned in the first one-third of the floor length.
(6) The maximum reduction in relative scour length is achieved by using a single row of rasp heads at 0.67 of the floor lengths, yielding a reduction ratio of 92.84% at Froude number equal to 0.19.
(7) The placement of a single line of rasp heads in the first one-third of the downstream floor results in the greatest reduction in scour length compared with the flat floor, except at Froude numbers of 0.33 and 0.19.
(8) Generally, the scour hole dimensions along the flume's centerline in the case of rasp heads in

three positions are smaller than those observed in cases involving four relative heights of the end sill and a flat floor.

(9) Nonlinear regression relations have been developed to simulate the experimental results for maximum scour depth and length. The predicted results closely match the experimental findings with only minor discrepancies.

Overall, these findings provide valuable insights into the effectiveness of different energy dissipators and their impact on mitigating local scour downstream of hydraulic structures, offering practical guidance for future engineering applications.

6.1. Recommendations

It is recommended to:

(1) Study a fully floored weir with rasp heads arranged in lines of staggered to determine their effect on scour hole downstream of weirs.

(2) Study the scour phenomenon downstream of weirs using different types of soil to estimate the effect of soil characteristics on this phenomenon underusing the rasp heads.

Funding

There are no funders or grand IDs for my research.

Author contributions

Hadeer Abdelati: Conceptualization, Methodology, Experimentation, Writing-original draft.

EL-Masry, A.A.: Conceptualization, Methodology, Supervision, Review.

Shamaa, M.T.: Conceptualization, Methodology, Experimentation, Formal analysis, Writing-review & editing.

Nassar, K.A.: Writing-review the scientific content & editing, Making adjustments to the language.

Conflict of interest

I declare that there are no potential conflicts of interest with respect to the research authorship or publication of this article.

Notation

B	channel width
b	weir crest width
h	weir height
H_w	head at the rectangular weir in the inlet tank
H	head above weir crest
H_s	scour head
d_{sm}	maximum scour depth
L_{sm}	maximum scour length
y_2	tail water depth
L_f	floor length
Q	water discharge
V	water velocity
ρ	water density
μ	water viscosity
d_{50}	mean particle diameter
g	gravity acceleration
p_s	sediment density
σ	standard deviation of bed material
h_s	end sill height
L_s	end sill length
L	position of rasp heads row from the weir
S	distance between rasp heads
h_b	rasp head height
L_b	rasp head length
W_b	rasp head width
F.F	flat floor without energy dissipation
E.S	end sill
R.H	rasp heads

References

Abdallah, M., 1990. Study of Local Scour for Channel Bed Downstream Heading-Up Structure [MSc Thesis]. Mansoura. Mansoura University, Egypt.

Abdel Samad, H., Helal, Y.E., Ibrahim, S., Sobeih, M., 2012. Minimizing of scour downstream hydraulic structures using semi-circular sill. Eng. Res. J. 35, 129–137.

Abdelhaleem, F.S.F., 2013. Effect of semi-circular baffle blocks on local scour downstream clear-overfall weirs. Ain Shams Eng. J. 4, 675–684.

Abozeid, G., Ibrahim, H., Shehata, S.M., 2010. Hydraulics of clear overfall weirs with bottom openings. J. Eng. Sci. 38, 19–28.

Alaa, N., Abdel-Mageed, N.B., Ali, A.M., Mahgoub, E.S., 2021. Studying the Best Location and Dimensions of the Stilling Basin Pool Downstream Hydraulic Structures.

Alabas, M.A.A.A., Al-Ameri, R., Chua, L., Das, S., 2017. 65 Investigation of Energy Dissipation in Gabion Stepped Weirs and HCED Iraqi Scholars Conference in Australasia, vol. 2017.

Alikhani, A., Behrozi-Rad, R., Fathi-Moghadam, M., 2010. Hydraulic jump in stilling basin with vertical end sill. Int. J. Phys. Sci. 5, 25–29.

Amin, A.M.A., 2015. Physical model study for mitigating local scour downstream of clear over-fall weirs. Ain Shams Eng. J. 6, 1143–1150.

Awaad, A.S., 2023. Investigation of using a sill under the gate as a scour countermeasure downstream of a sluice gate. Egypt Int J Eng Sci Technol 43, 74–80.

Bestawy, A., Hazar, H., Ozturk, U., Roy, T., 2013. New shapes of baffle piers used in stilling basins as energy dissipators. Asian Trans. Eng.Egypt Int. J. Eng. Sci. Technol. 3, 1–7.

Bormann, N.E., Julien, P.Y., 1991. Scour downstream of grade-control structures. J. Hydraul. Eng. 117, 579–594.

Chaudhary, R.K., Ahmad, Z., Mishra, S.K., 2022. Scour downstream of a corrugated apron under wall jets. Water Pract. Technol. 17, 204–222.

Dargahi, B., 2003. Scour development downstream of a spillway. J. Hydraul. Res. 41, 417–426.

D'agostino, V., Ferro, V., 2004. Scour on alluvial bed downstream of grade-control structures. J. Hydraul. Eng. 130, 24–37.

El-Gamal, M.M., 2001. Effect of using three-lines of angle baffles on scour downstream heading-up structures. Mansoura Eng. J. 26, 73–85.
El-Mahdy, M.E.-S., 2021. Experimental method to predict scour characteristics downstream of stepped spillway equipped with V-Notch end sill. Alex. Eng. J. 60, 4337–4346.
El-Masry, A., 2001. Minimization of scour downstream heading-up structures using double line of angle baffles. In: Proc of Sixth International Water Technology Conference (IWTC), Alexandria, Egypt.
El-Masry, A., Sarhan, T., 2000. Minimization of scour downstream heading-up structure using a single line of angle baffles. Eng. Res. J. Helwan Univ. 69, 69.
Elnikhely, E.A., Fathy, I., 2020. Prediction of scour downstream of triangular labyrinth weirs. Alex. Eng. J. 59, 1037–1047.
Farhoudi, J., Shayan, H.K., 2014. Investigation on local scour downstream of adverse stilling basins. Ain Shams Eng. J. 5, 361–375.
Hamed, Y., El-Kiki, M., Mirdan, A., 2009. Scour downstream oblique V-notch weir. In: Thirteenth International Water Technology Conference. IWTC, Hurghada, Egypt, pp. 853–872.
Hamidifar, H., Nasrabadi, M., Omid, M., 2018. Using a bed sill as a scour countermeasure downstream of an apron. Ain Shams Eng. J. 9, 1663–1669.
Helal, E., Nassralla, T., Abdelaziz, A., 2013. Minimizing of scour downstream hydraulic structures using sills. Int. J. Civ. Struct. Eng. 3, 591.
Hong, S., Biering, C., Sturm, T.W., Yoon, K.S., Gonzalez-Castro, J.A., 2015. Effect of submergence and apron length on spillway scour Case Study. Water 7, 5378–5395.
Kang, J.-G., 2017. An experimental study on the dissipation effect of a baffle downstream of a weir. Engineering 9, 937–949.
Karimi Chahartaghi, M., Nazari, S., Solimani Babarsad, M., 2022. Experimental and numerical investigation of the effect of diverging sidewall of baffled apron with semi-circle blocks on the energy dissipation and scour hole dimension at downstream. Iran J. Sci. Technol. Trans. Civil Eng. 46, 1405–1419.
Melville, B.W., Sutherland, A.J., 1988. Design method for local scour at bridge piers. J. Hydraul. Eng. 114 (10), 1210–1226.
Obaida, A.A.M., Khattab, N.I., Mohammed, A.Y., 2023. Scour depth downstream sharp-crested weir. J. Eng. Appl. Sci. 70, 1–11.
Rashed, R.E., El-Masry, A.A., Abdelgawad, H.A.A., 2022. Effect of hollow semi-circular baffles arrangement on local scour downstream hydraulic structures. Mansoura Eng. J. 47, 22–31.
Varaki, M.E., Sedaghati, M., Sabet, B.S., 2022. Effect of apron length on local scour at the downstream of grade control structures with labyrinth planform. Arabian J. Geosci. 15, 1240.
Wang, F., Chen, X.-Q., Chen, J.-G., 2017. Experimental study on the energy dissipation characteristics of debris flow deceleration baffles. J. Mountain Sci. 14, 1951–1960.
Wu, C.M., 1973. Scour at downstream end of dams in Taiwan. Sediment Transp. 1.
Zahed, E., Farhoudi, J., Javan, M., 2010. Similarity of scour evolution downstream of stilling basin with an end sill. New Aspects of Fluid Mechanics. Heat Tran. Eng.